Application of Robust Control to Chatter Attenuation for a High-Speed Machining Spindle on Active Magnetic Bearings

Alexander H. Pesch and Jerzy T. Sawicki*
Center for Rotating Machinery Dynamics and Control
Cleveland State University
Cleveland, OH, USA

Abstract

The purpose of this work is to demonstrate a robust control strategy to avoid machining chatter in a high-speed machining spindle levitated on active magnetic bearings. Chatter avoidance is an important aspect in machining because chatter limits the material removal rate and inhibits production. A method is implemented which uses μ-synthesis AMB control with a cutting force model in the controller design process. Such an approach causes the controller to stabilize the naturally unstable cutting process, avoiding chatter and resulting in smoother surface finish, longer tool life and increased material removal rate. Stability lobe diagrams are calculated for the new control strategy showing increased critical feed rate and confirmed through numerical simulations. The developed method is implemented experimentally on the high-speed AMB machining spindle. Impulse hammer testing is performed to measure the controlled spindle's transfer function and evaluate chatter free machining suitability.

1 Introduction

Machining chatter is often the most limiting factor in material removal rate (MRR). Chatter is an unstable vibration of the cutting tool which occurs when machining with too severe of a feed rate. Chatter results in a poor surface finish, the inability to hold dimensional tolerance, accelerated tool wear and in severe cases tool breakage. Any increase in the feed rate threshold for chatter will translate to increased MRR and therefore higher productivity in machining operations. Productivity in machining is a critical issue because machining is very costly. Machining operations in production are estimated to cost over $250 billion per year [1] to American industry alone.

Traditionally, machinists are limited in dealing with chatter by decreasing the feed rate or manually looking for a "sweet spot" cutting speed, where chatter will not occur [2]. Making this process automated in feedback is the basic level of active chatter control [3]. This automation may be more convenient but does not offer any advantages in terms of increasing the maximum possible MRR. It is also heuristically known that a tool holder with more damping and higher dynamic stiffness will be less likely to chatter. Active magnetic bearings (AMBs) provide the opportunity to avoid chatter through intelligent control [4]. Additionally, a spindle built on AMBs has the advantages of non-contact support such as increased speed and wider spindle diameter.

As most machining setups are not built on magnetic bearings most research efforts in the area of active chatter control have been for non-AMB systems augmented with actuators. Non-AMB machining systems have been fitted with actuators, such as piezoelectric pads [5], electrostrictive elements [6], active mass dampers [7], or magnetic actuators [8]. These types of actuators have been controlled using various methods, including LQR [6, 8], H_∞ [7] or μ-synthesis [5]. The design criteria for control of these actuators have been maximizing the dynamic stiffness and/or adding active damping to the machining setup. These criteria result from the observation that systems with high dynamic stiffness have better chatter limits than systems with low dynamic stiffness, and systems with high damping have better chatter limits than systems with low damping. High stiffness results in small deflections for a given force and damping removes energy from a vibrating system. These active approaches are applied to systems that cannot achieve satisfactory chatter limits through structural design, for example a slender boring bar.

A conceptual leap beyond previous methods is the addition of a cutting force model in the controller synthesis. The significant advantage of this addition is that the controller will also stabilize the chatter, in addition to

*j.sawicki@csuohio.edu, Cleveland State University, Department of Mechanical Engineering, 2121 Euclid Ave., SH 248, Cleveland, OH 44115, Phone: 216.687.2565, Fax: 216.687.5375

stabilization of the AMBs. Therefore, such an approach will design a controller specifically for chatter prevention rather than just tuning a system parameter known to improve chatter, such as dynamic stiffness.

There have been a number of studies on μ-synthesis control of chatter using a cutting model. In 1993 Kashani et al. [9] performed calculations for a lathe with the cutting tool modeled as a lumped mass-spring system and the actuator as a single force on the cutting tool. The authors concluded that the robust control scheme showed potential for minimizing the vibrations in a turning process. In 2007, Chen and Knospe [10] performed an experimental study on a lathe in which the tool holder was supported with an active magnetic actuator. A 63% increase in limiting stable chip width was achieved by using μ-synthesis control instead of PID control. In 2010, van Dijk et al. [11] performed a numerical study for a milling spindle on ball bearings. The controlled actuator was modeled as a force on the milling head in the two directions perpendicular to the spindle axis. The authors found that similar increase in the critical chatter limit can be achieved for a high-speed rotating system. In 2012, van Dijk et al. [12] extended their work with the consideration of a magnetic actuator.

This paper presents the development and application of μ-synthesis control with an embedded force cutting model for attenuation of chatter. The control scheme is applied to a five-axis controlled machining spindle supported on active magnetic bearings. Section 2 addresses the chatter attenuation approach with an overview of μ-synthesis and an explanation of the application of the cutting model. Section 3 describes the application of the chatter attenuation method to an experimental AMB high-speed machining spindle. For comparison, two controllers are designed: the *chatter avoiding controller* designed using the cutting force model and the *dynamic stiffness controller* designed to maximize the spindle's dynamic stiffness. Section 4 presents the controllers resulting from both design methods. Section 5 presents the calculation of stability lobe diagrams and numerical time simulation of machining using both controllers. Section 6 covers experimental implementation of the two controllers on the spindle. Impact hammer testing is performed to measure the levitated spindle's transfer function at the tool location. These transfer functions are used to evaluate suitability for chatter free machining. Section 7 concludes the paper with a summary of the findings.

2 Description of Method

2.1 μ-Synthesis

AMB systems for rotating machinery represent a classic challenge for multi-input, multi-output (MIMO) control. An AMB-rotor system inherently involves multiple interacting control mechanisms and many conflicting performance objectives. For these reasons, AMB-rotor systems are a perfect application of modern robust MIMO control design techniques such as μ-synthesis, which simultaneously addresses stability and robustness in a systematic design procedure.

The AMB system may be described by the block diagram in Figure 1. The plant to be controlled, *G*, is the rotor, AMBs and power amplifiers. The control inputs *u* are signals delivered to the power amplifiers, the measurements *y* are signals received from position sensors, the loads *w* are external forces or electrical noise acting on the system, and performance measures *z* are those signals that the engineer will monitor in assessing adequate management of the loads *w*. Essential to μ-synthesis is an assumption that the mapping *G* is linear time invariant (LTI). Also, it is common to model the controller as LTI for the bulk of the design and analysis work. As such, the controller may be described by a matrix transfer function *H*. The closed-loop system is shown in Figure 1.

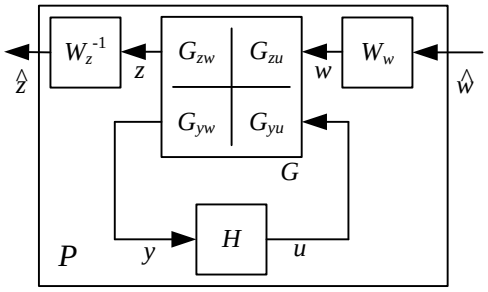

Figure 1: AMB system with controller closed-loop

Equation (1) maps the non-dimensional exogenous signals $\hat{w}$ to the non-dimensional performance measures $\hat{z}$.

$$\hat{z}(s) = P\hat{w}(s) \tag{1}$$

where P is the weighted closed-loop performance function:

$$P = W_z^{-1}\left[G_{zw} + G_{zu}H\left(I - G_{yu}H\right)^{-1} G_{yw} \right] W_w \tag{2}$$

When the plant model satisfies the LTI assumptions and the performance objective is to ensure that the peak gain of P is less than some target threshold, γ, then the problem is one of H_∞ control and synthesis is accomplished by the sole additional step of delivering the weighted model to the algorithm to perform H_∞ synthesis.

An additional consideration in controller design is that the behavior of G may not match the actual plant. The actual plant G_p may be better described by the nominal plant G_0 in combination with some specific uncertainty perturbation, Δ. Figure 2 shows the model structure of Figure 1 amended to include this perturbation.

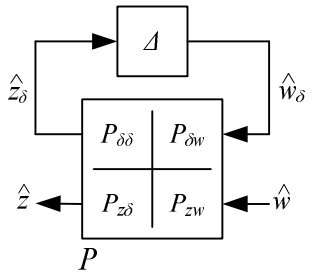

Figure 2: Model with uncertainty

It is assumed that the actual values of the elements of G_p are not known but that they are bounded by $\Delta \in \mathbf{\Delta}$ where we the structure of $\mathbf{\Delta}$ is known and its elements are bounded. As a result, the control problem becomes: ensure that the closed-loop system is stable and that $|P|_\infty < \gamma$, for all $\Delta \in \mathbf{\Delta}$. This case is a μ-synthesis problem. As in the previous case, the solution strategy is to specify the nominal plant G_0, the target gain bound γ, and the uncertainty set $\mathbf{\Delta}$. When these three elements are submitted to the computational machinery of μ-synthesis, the required controller is produced automatically, if one can be formulated to meet the specifications [13].

2.2 Provisions for Chatter

In this work, the linear machining force model of Tobias [14] is used,

$$f_r = k_c l(e_0 + v(t) - v(t-\tau)) \tag{3}$$

where f_r is the radial component of the cutting force, l is the length of the chip perpendicular to the direction of tool vibration, e_0 is the nominal cut width, $v(t)$ is the radial tool position during the current machining pass, and $v(t\text{-}\tau)$ is the radial tool position for the previous machining pass. The time τ between one machining pass and the next is a function of rotation speed of the spindle (or, of the workpiece, in the case of a lathe). The constant k_c is cutting stiffness which is the coefficient relating the chip area to the cutting force in the radial direction. Cutting stiffness depends on many factors such as workpiece material and tool geometry. The area of the chip is the length of the chip times the width of the chip. The length of the chip is the linear distance that the tool feeds in one revolution of the spindle or workpiece. This length is fixed by the machining feed rate. The width of the chip is the nominal width, the depth of cut set by the operator, e_0, plus the vibration of the tool, $v(t)$, minus the vibration of the tool which created the overlaying surface $v(t\text{-}\tau)$. The resulting chip width is shown schematically in Figure 3. Note that the chip length l is measured into the page. This model has gained wide acceptance for its explanation of machining chatter through the so called regenerative effect.

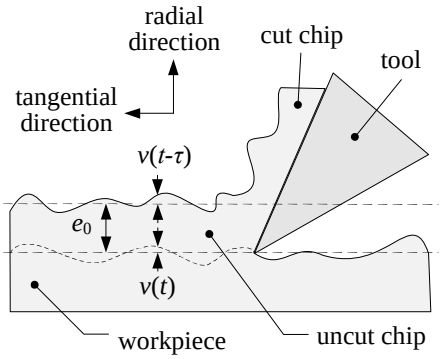

Figure 3: Diagram showing tool cut width and regenerative mechanism

The tool is attached to the flexible spindle, which has its own dynamics. The cutting force on the tool is a position feedback similar to stiffness. The presence of the delay term in Equation (3) gives rise to the potential for instability in the closed-loop machining system. For a given delay time, τ, there exists a feedback gain (given by k_c and l) large enough that variations in the chip width cause vibrations of the tool to grow with each pass. Specifically, the functions $v(t)$ and $v(t-\tau)$ will either be in phase or out of phase depending on the dynamics of the spindle and the delay time. If they are in phase the magnitude of chip width will be constant with time. If they are out of phase the magnitude of the chip width will oscillate. Because the cutting force is proportional to chip area an out of phase $v(t)$ and $v(t-\tau)$ will drive even greater vibrations for the next pass. Therefore, machining chatter is a self-excited vibration. Such an instability can be corrected by model based controls techniques. For a more complete discussion on the mechanism of regenerative chatter, see [15].

The model based robust control approach of μ-synthesis discussed in the previous section can be used to combat machining chatter. This is done by augmenting the typical model used in AMB controller design by including the cutting force model shown in Equation (3). The robust controller will stabilize the machining chatter along with the magnetic bearing instability. Figure 4 shows an example block diagram of a machining system used for μ-synthesis. The figure shows how the plant is augmented to include the cutting force model. The uncertainty blocks illustrate that the original tool system and the cutting force model have their own parametric uncertainties, which are maintained when augmenting the plant model for robust chatter control. The specific uncertainties used in the application of the chatter avoiding method to the high-speed AMB machining spindle are discussed in the next section.

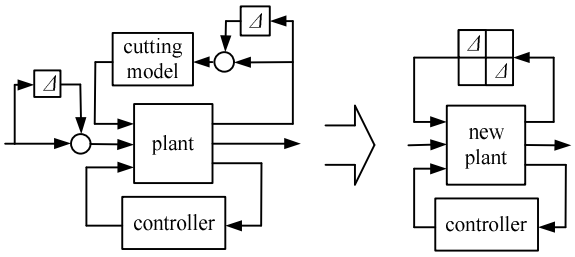

Figure 4: Conceptual block diagram of augmenting system plant with cutting force model for chatter avoiding μ-synthesis controller design

3 Application to AMB Spindle

An industrial grade AMB high-speed machining spindle is the platform for this research. Figure 5 shows a photograph and cross section of the AMB spindle. The spindle was developed by SKF Magnetic Bearings Inc. for single point boring with the spindle housing fixed and the workpiece held in a movable chuck. The spindle is supported by two radial AMB's and one thrust AMB. The static load capacity is approximately 1400 N for the front radial bearing, 600 N for the back radial bearing, and 500 N for the thrust bearing. An AC electric motor is situated

between the bearings so that no additional motor bearings are needed. The motor can drive the spindle up to 50,000 RPM at 10 kW. For real time implementation of experimental AMB controllers a dSPACE DS1005 PPC board with DS2001 A/D and DS2101 D/A converters are used.

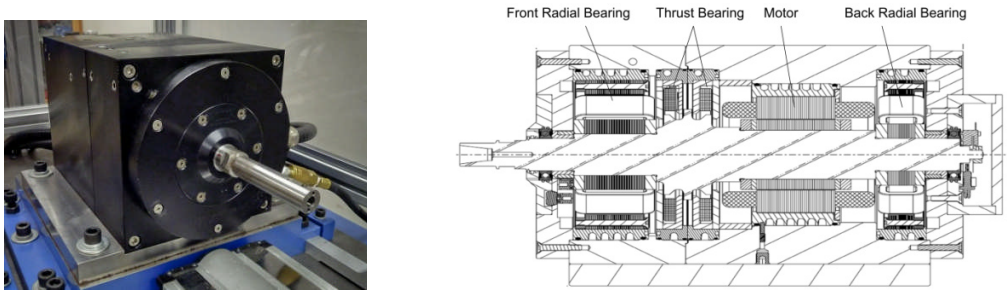

Figure 5: Photograph of AMB machining spindle (left) and cross section spindle of without tool holder (right)

The plant model of the spindle system includes models of the components i.e., rotor, PWM power amplifiers, digital hardware, and actuators. All of the components are experimentally identified and validated. The model of the power amplifiers includes the digital hardware and inductive load of the AMB coils. The power amplifier model is created by performing a current signal sine sweep and fitting the data using MATLAB's system identification toolbox. The AMB actuators are modeled as a force which varies linearly with control current and rotor position. The current stiffness, k_i, and position stiffness, k_x, are identified through incremental application of static loads to the spindle, which is levitated with an initial controller. An arbitrary controller such as PID can be used in identification, provided it utilizes the same bias current as the final μ-controller. Changes in the steady state control current vs. load are used to find current stiffness, and changes in controller set point vs. the product of the resulting control current and current stiffness are used to find position stiffness [16]. The open-loop plant model is assembled as shown in Figure 6 (left). Note that the signals are 4×1 vectors for the four radial control axes. The open-loop plant is identified by levitating the rotor with an initial controller and performing a control current perturbation sine sweep. The open-loop transfer functions are extracted from the closed-loop measurements in the same manner as in [17]. The rotor has previously been modeled with the finite element method and the model was updated numerically to match open-loop plant data [18]. Figure 6 (right) shows a comparison of the Bode plots of the open-loop model and experimental sine sweep. Two control axes are shown for the front and back bearings in a single plane giving 4 transfer functions. Only 4 plots are shown because the spindle is axially symmetric. The spindle first flexible mode is 1070 Hz and the second flexible mode is 1970 Hz.

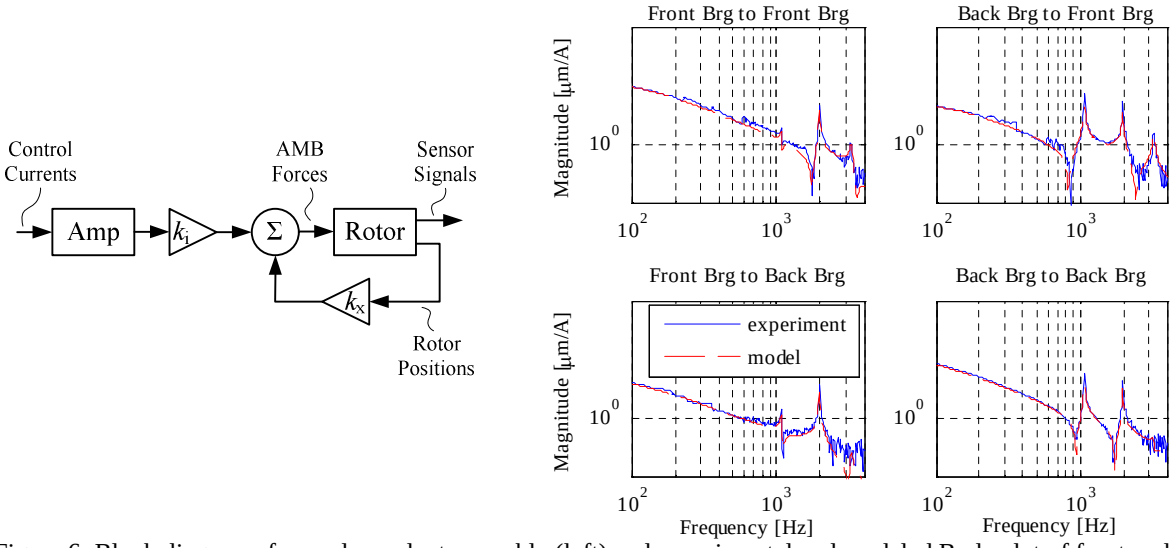

Figure 6: Block diagram of open-loop plant assembly (left) and experimental and modeled Bode plot of front and back bearing control axes (right)

To design a μ-controller for the AMBs with no machining, the considered plant model must have weighted performance inputs for bearing loads, and sensor noise along with weighted performance outputs for rotor deflection at the bearing location and control current. The specifications of the bearing load frequency dependent performance weights are given in Table 1. The bearing deflections are limited to 50 µm above 0.002 Hz, and to 1 µm below 0.002 Hz. The maximum control current is 4 A, with a performance weight roll off at 1 kHz as to not saturate the current amplifiers. For robustness to broadband sensor noise disturbance, noise is modeled as a constant 0.9 µm gain across all frequencies. The actual noise level of the eddy current position sensors in the AMBs is under 0.6 µm, but it is found that setting a more severe noise performance weight is helpful in obtaining μ-controllers that are open-loop stable. An open-loop unstable controller can achieve the design criteria as long as the closed-loop is stable. However, it is advantageous for practical implementation to have an open-loop stable controller.

	tool tip end	drive end
DC Load	300 N	130 N
first break	0.001 Hz	0.001 Hz
midfrequency load	80 N	50 N
second break	40 Hz	40 Hz

Table 1: Bearing Load Parameters

When designing a μ-controller for the AMBs with machining, performance weights are needed for the machining in addition to the weights for levitation. The dynamic stiffness controller is designed with no cutting model in the plant, but there is a performance input for load at the cutting tool. The tool load input is needed to bring about stiffness at the tool. The maximum load for high-speed machining is set at 27 N. This load rolls off over the range of machining speed up to 833 Hz (50,000 RPM). The chatter avoiding controller accounts for the cutting force by including the cutting model Equation (3) in the plant model. For the chatter avoiding control scheme there is no tool load input but only a nominal cut width input. The maximum nominal cut width is weighted at 50 µm over the frequency range of machining. For both control schemes the tool deflection is limited to 25 µm over the frequency range of machining.

The uncertainties used in μ-synthesis controller design are summarized in Table 2. The model running speed is set at half the maximum running speed with a real multiplicative uncertainty of ±100%, to cover the entire operating range of the spindle. Two additional uncertainties are needed for the cutting model. The first is the cutting stiffness, which must vary from zero to the maximum stiffness. This ensures that the resulting controller can levitate the rotor and rotate to speed with or without cutting. The second uncertainty is a unity bounded complex uncertainty which takes the place of the unknown delay in the machining process [10]. This time delay is unknown because the running speed is uncertain. The complex uncertainty represents all possible time delays since its magnitude is one, encompassing all possible phase shifts.

Uncertainty	Type	Nominal	Range
Running Speed	Real	25,000 RPM	±100%
Cutting Stiffness (only for cutting model)	Real	$1.4\times10^{9}\ \frac{\mathrm{N}}{\mathrm{m}^2}$	±100%
Delay (only for cutting model)	Complex	0	Radius = 1

Table 2: Uncertainties used in controller design

Both the chatter avoiding method and the dynamic stiffness method are maximized by tuning a single parameter in their respective controller design schemes. The performance weight for the tool load is maximized, while the dynamic stiffness controller maintains robust stability. By using the largest possible tool load in the design process, the dynamic stiffness is maximized. The cutting stiffness uncertainty is maximized, while the chatter avoiding controller maintains robust stability. By using the largest possible cutting stiffness uncertainty, the range of chatter free machining is maximized. All other performance weighting and uncertainty parameters are held constant during the tuning. All model parameters not directly related to the cutting model or tool load are constant for chatter avoiding method and dynamic stiffness method.

4 Controller Design Results

Two μ-synthesis controllers are designed for the spindle's AMBs. The chatter avoiding controller uses a plant including a cutting force model such that the resulting system is robust to the instability of machining chatter. The dynamic stiffness controller is designed to maximize the tool's dynamic stiffness and represents the current state-of-the-art. The μ-controllers are synthesized by D-K iteration [18] in MATLAB using the *dksyn* command. The results of the two controller designs are shown in Figure 7. Each μ-controller has 4 cross coupled control axes, two for each radial AMB. Figure 7 shows four input-output pairs for a single physical plane.

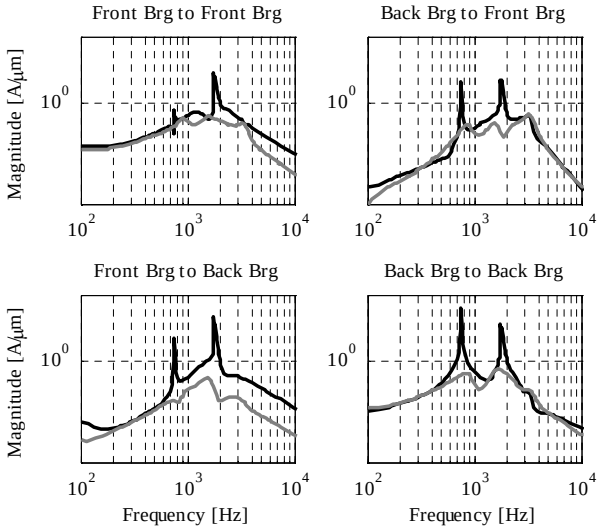

Figure 7: Magnitude of the FRF of the controllers obtained by D-K iteration for the AMB spindle model including cutting model (black) and not including cutting model (grey)

Overall, the controller responses are similar. However the chatter avoiding controller has peaks at 754 Hz and 1840 Hz present in all control axes. The significance of these peaks is shown in the chatter frequency calculations in the next section.

5 Simulation Results

Two methods are used to evaluate the controllers before experimental implementation. The first is a projection of a stability lobe diagram (SLD) for the spindle using each controller. The SLD is a well known tool in machining which plots the stability limit vs. rotation speed. The SLD is created by first using the nominal model with no cutting force with each of the designed controllers to make two closed-loop spindle models. Next, a cutting force model is added with a discrete value for feed rate and rotation speed. A 30^{th} order Padé approximation is used for estimating the time delay. Beginning at zero running speed and feed rate, the eigenvalues of the system are calculated and used to evaluate stability. If the system is stable, the discrete feed rate is increased by one step and a new model is assembled and stability checked. If the system is unstable, the feed rate is reset to zero and the running speed is increased by one discrete step. In this manner the nominal SLD is constructed point by point for each controller. The feed rate increment used is 10 µm and the spindle speed increment used is 500 RPM. The resulting stability lobes are shown in Figure 8. The curve indicates the boundary of stability. The boundary is higher for the chatter avoiding controller than for the dynamic stiffness controller, indicating superior machining performance.

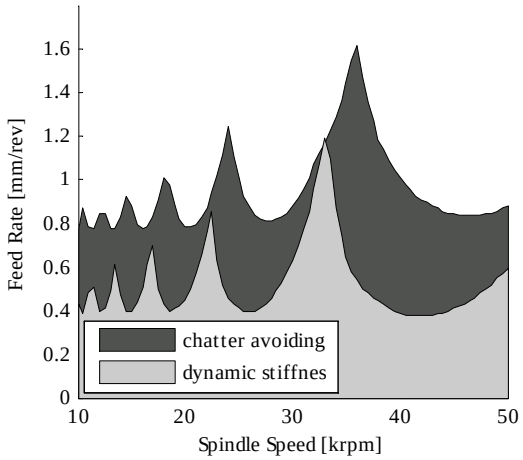

Figure 8: Stability boundary calculated for using the controllers developed with and without the cutting force model

Next, the eigenvalues at the border of stability are used to find the chattering frequency. This gives additional insight into the dynamics of chatter attenuation. Figure 9 (left plot) shows the frequency of the single eigenvalue at the border of stability. This is the speed dependent chatter frequency and is plotted vs. spindle speed, similarly to the SLD shown in Figure 8. The abrupt jumps in chatter frequency occur when moving from one stability lobe to the next. Regardless of spindle speed, the chatter frequency is bounded, as indicated by the shaded region. This range falls after the first sharp peak, which occurs in the chatter avoiding controller but is not present in the dynamic stiffness controller, as shown in the right plot of Figure 9. This range of chatter frequency is associated with the first flexible mode of the spindle. There is the possibility of chattering associated with the second flexible mode of the spindle at over 2 kHz. This chatter is not seen at the border of stability because it is the primary mode of chatter that occurs at the critical feed rate. If the feed rate were increased past the critical feed rate the second mode of chatter could be seen as well. The possibility of the second mode of chatter explains the second chatter avoiding controller peak.

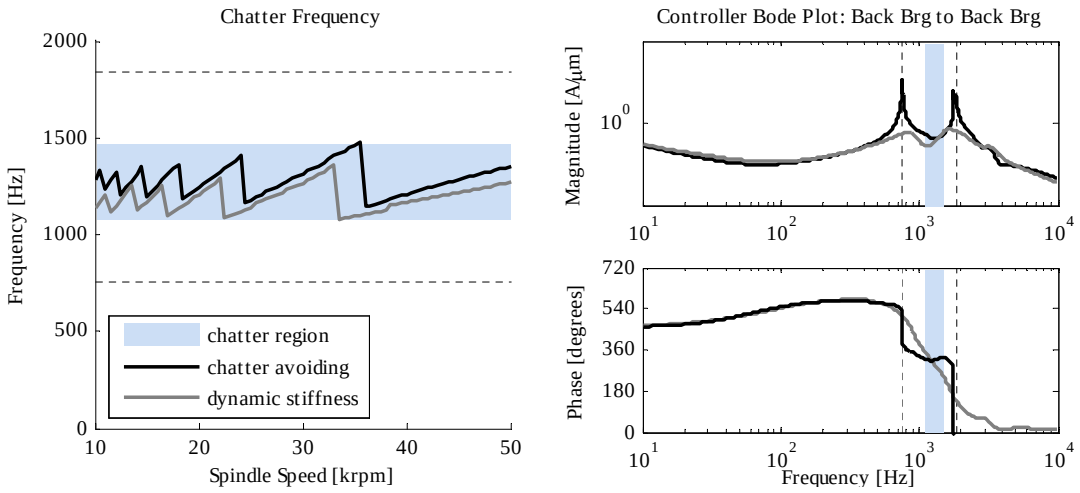

Figure 9: Chatter frequency vs. spindle speed at critical feed rate (left) and Bode plot of chatter avoiding and dynamic stiffness controllers for back bearing with chatter frequency range shaded (right)

The second controller evaluation is a numerical time simulation of the machining process. The simulation is of machining with a constantly increasing feed rate such that the feedback force gain on the tool increases linearly with time. The simulation is completed in MATLAB using a variable step size numerical integration. A numerical delay is used for the time delay in the machining force. The parameters of the simulation are shown in Table 3. The value for cutting stiffness of aluminum is taken from [20].

Parameter	Value	Unit
Speed	40,000	RPM
Material	Aluminum	NA
Cut Stiffness	1×10^{-3}	$N/\mu m^2$
Nominal Cut	100	µm
Feed Rate	0-1.25	mm/rev

Table 3: Parameters used in cutting simulation

The simulation is repeated for each controller. Figure 10 shows time plots of the simulation results for each controller. The vibration of the tool and the feed rate are shown vs. time. Chatter occurs at the critical feed rate, as indicated by an abrupt increase in vibration amplitude. It can be noticed that in the case of the chatter avoiding controller, the chatter occurs at a higher feed rate. This result indicates that the chatter avoiding controller is superior for machining and is in agreement with the projected SLD's.

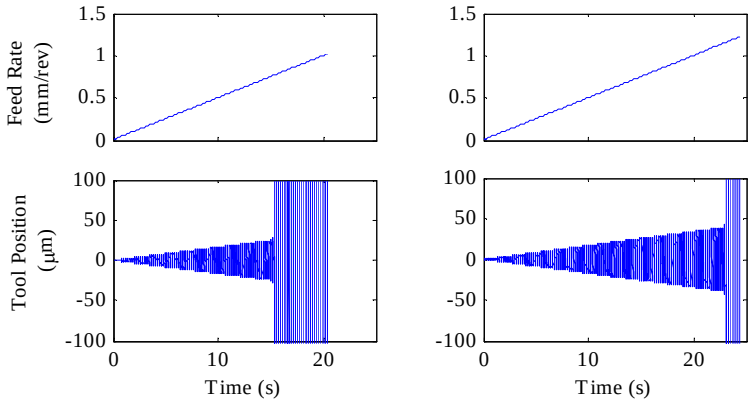

Figure 10: Cutting simulation results for dynamic stiffness μ-controller (left) and chatter avoiding μ-controller (right). Chatter presents as a rapid increase in tool vibrations at the critical feed rate.

6 Experimental Results

Both, the chatter avoiding and dynamic stiffness μ-controllers are experimentally implemented on the spindle. To evaluate machining ability the spindle's transfer function is measured through impulse hammer testing. Figure 11 shows a photograph of the hammer test.

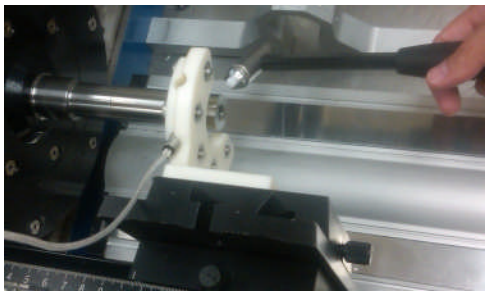

Figures 11: Impulse hammer experimental setup showing close up of impact area with hammer held in position

The force transducer is inside a PCB Piezotronics impulse hammer 086C03. The displacement transducer is a Lion Precision capacitance probe C23-C with driver CPL290. The data is collected and processed via a HP dynamic signal analyzer 35670A.

It is widely accepted that the real part of the tool's transfer function gives the limiting stable cutting conditions, according to the following equation [21]:

$$(k_c l)_{\min} = \frac{-1}{2(-1)\max\left|(\mathrm{Re}(P_0))\right|}, \quad \mathrm{Re}(P_0) < 0 \tag{4}$$

Here k_c and l are the cutting stiffness and chip length, respectively. P_0 is the levitated spindle transfer function at the tool location. Equation (4) is based on the Nyquist stability criteria. According to the Nyquist stability criteria, the machining system will be on the border of chatter stability if the opened-loop has a complex response that passes through the point -1+0j but does not encircle it [22]. In this case, the opened-loop is $P_0 k_c l(1-e^{-sT})$ which is the levitated spindle, P_0, cascaded with the cutting force, Equation (3), in the Laplace domain. This expression of the Nyquist stability criteria can be used because the opened-loop is stable. Individually, the levitated spindle is stable, the cutting stiffness is stable, and the delayed cutting stiffness is stable, therefore the combination of these is stable. By setting the opened-loop response to -1+0j for an arbitrary delay time and rearranging, Equation (4) is found. Therefore, maximizing the most negative real part of the spindle transfer function, P_0, maximizes the chatter-limiting cutting stiffness or chip length, below which chatter will not occur at any speed. Figure 12 shows the measured transfer function P_0, magnitude vs. frequency (left), and imaginary vs. real parts (right). Measurements using the chatter avoiding and dynamic stiffness controllers are shown. The 39% increase in most negative real part indicates a 39% increase in the chatter limiting feed rate.

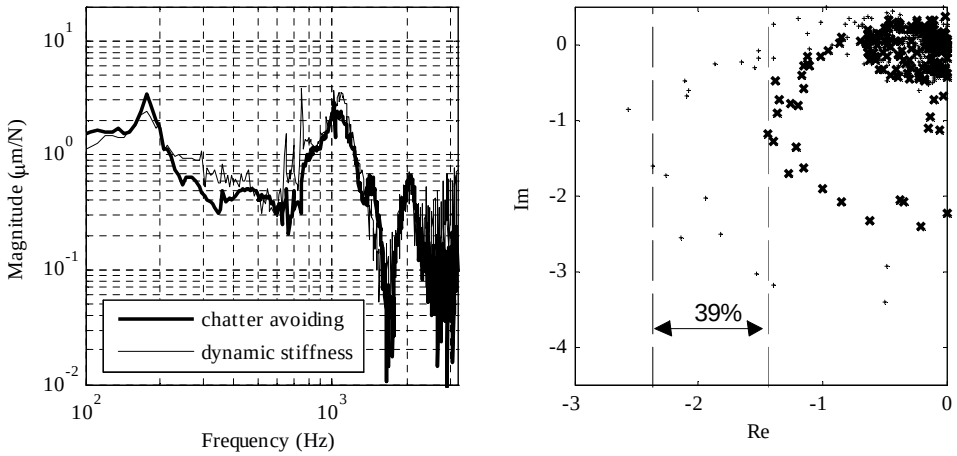

Figure 12: Tool's compliance for chatter avoiding (thick) and dynamic stiffness (thin) μ-controllers – magnitude as a function of frequency (left) and complex gain (right)

7 Conclusions

A μ-synthesis controller has been designed for the AMBs supporting a high-speed machining spindle for the specific purpose of avoiding machining chatter. This was acomplished by incorporating a cutting force model into the overall system model used for controller synthesis. The chatter avoiding μ-controller is compared to a μ-controller designed to achieve high dynamic stiffness at the tool, which represents the current state-of-the-art. Stability lobe diagrams were calculated and numerical time simulations of machining were conducted using both controllers. An improvement in limiting stable feed rate is achieved. Both controllers were experimentally implemented on the AMB spindle. Impulse hammer tests were conducted to measure the spindle's transfer function at the tool location. The measurements show a 39% improvement in the real part of the tool transfer function. This translates to a 39% increase in the chatter free feed rate. The higher possible chatter free feed rate leads to higher MMR, speeding up production.

Acknowledgements

This work was supported by the Cleveland State University Research Council's Doctoral Dissertation Research Expense Award and Fellowship (DDREAFP) Program.

References

[1] C. Knospe. Active Magnetic Bearings for Machining Applications. *Control Engineering Practice*, 15, 2007.
[2] Sandvik Coromant. *Modern Metal Cutting*. Sweeden: Tofters Tryckeri AB, 1996.
[3] S. Tsai, K. Eman, and S. Wu. Chatter Supression in Turning. In *Proceedings of the 11th North American Manufacturing Research Conference NAMRC XI*, 1983.
[4] J. Kyung and C. Lee. Controller Design for a Magnetically Suspended Milling Spindle Based on Chatter Stability Analysis. *JSME International Journal, Series C*, 46(2), 2003.
[5] C. Ehmann, U. Schonhoff, and R. Nordmann. Active Damping for Gantry Milling Machines. In *8th International Congress on Sound and Vibration*, Hong Kong China, 2001.
[6] J.L. Dohner, J.P. Lauffer, T.D. Hinnerichs, N. Shankar, M. Regelbrugge, C-M Kwan, R. Xu, B. Winterbauer, and K. Bridger. Mitigation of Chatter Instabilities in Milling by Active Structural Control. Technical report, Sandia National Laboratories, SAND2001-3031, 2001.
[7] M. Marra, B. Walcott, K. Rouch and S. Tewani. H_∞ Vibration Control for Machining Using Active Dynamic Absorber Technology. In *Proceedings of the American Control Conference*, Seattle WA, USA, June, 1995.
[8] B. Späh, S. Kern, R. Nordmann, and S. Rinderknecht. Optimal Control of Chatter Vibration of a Motor Spindle with Integrated Electromagnetic Actuator. In *Proceedings of the 8th IFToMM International Conference on Rotordynamics*, Seoul Korea, 2010.
[9] A. Kashani, J. Sutherland, K. Moon, and J. Michler. A Robust Control Scheme for Improving Machined Surface Texture. In *Transactions of NAMRI/SME*, 21, Stillwater OK, USA, 1993.
[10] M. Chen and C. Knospe. Control Approaches to the Suppresion of Machining Chatter Using Active Magnetic Bearings. *IEEE Transactions on Control Systems Technology*, 15(2), March 2007.
[11] N. Dijk, N. Wouw, E. Doppenberg, H. Oosterling, and H. Nijmeijer. Chatter Control in the High-Speed Milling Process using Mu-Synthesis. In *2010 American Control Conference*, Baltimore, MD, USA, 2010.
[12] N. Dijk, N. Wouw, E. Doppenberg, H, Oosterling, and H. Nijmeijer. Robust Active Chatter Control in the High-Speed Milling Process. *IEEE Transactions on Control Systems Technology*, 20(4), July 2012.
[13] J.T. Sawicki and E.H. Maslen. Toward Automated AMB Controller Tuning: Progress in Identification and Synthesis. In *The Eleventh International Symposium on Magnetic Bearings (ISMB-11)*, Nara Japan, 2008.
[14] S. Tobias and W. Fishwick. A Theory of Regenerative Chatter. *The Engineer*, February 1958.
[15] Y. Altintas. *Manufacturing Automation Metal Cutting Mechanics, Machine Tool Vibrations, and CNC Design*. Cambridge University Press, New York NY, USA, 2000.
[16] R. Fittro, C. Knospe and L. Stephens. μ Synthesis Applied to the Compliance Minimization of an Active Magnetic Bearing HSM Spindle's Thrust Axis. *Machining Science and Technology*, 7(1), 2003.
[17] J. Sawicki and E. Maslen. Rotordynamic Response and Identification of AMB Machining Spindle. In *Proceedings of ASME Turbo Expo*, Montreal Canada, May 2007.
[18] A. Wroblewski, J. Sawicki and A. Pesch. High-Speed AMB Machining Spindle Model Updating and Model Validation. In *Proceedings of SPIE*, San Diego California, USA, March 2011.
[19] S. Skogestad and I. Postlethwaite. *Multivariable Feedback Control: Analysis and Design*. 2nd ed. John Wiley & Sons Ltd., Chichester England, 2005.
[20] J. Pratt and A. Nayfeh. Design and Modeling for Chatter Control. *Nonlinear Dynamics*, 19, 1999.
[21] R. King, Ed. . *Handbook of High-Speed Machining Technology*. Chapman and Hall, New York NY, USA, 1985.
[22] R. Dorf and R. Bishop. *Modern Control Systems*. Pearson Prentice Hall, Upper Saddle River NJ, USA, 2005.